Dalton Transactions

ROYAL SOCIETY OF CHEMISTRY

PAPER

View Article Online
View Journal | View Issue

Cite this: *Dalton Trans.*, 2022, **51**, 2400

Tungsten(VI) selenide tetrachloride, $WSeCl_4$ – synthesis, properties, coordination complexes and application of $[WSeCl_4(Se^nBu_2)]$ for CVD growth of WSe_2 thin films†

Victoria K. Greenacre, *[a] Andrew L. Hector, [a] Ruomeng Huang, [b] William Levason, [a] Vikesh Sethi[b] and Gillian Reid *[a]

$WSeCl_4$ was obtained in good yield by heating WCl_6 and Sb_2Se_3 *in vacuo*. Green crystals grown by sublimation were shown by single crystal X-ray structure analysis to contain square pyramidal monomers with apical W=Se, and powder X-ray diffraction (PXRD) analysis confirmed this to be the only form present in the bulk sample. Density functional theory (DFT) calculations using the B3LYP-D3 functional replicated the structure, identified the key bonding orbitals, and were used to aid assignment of the IR spectrum of $WSeCl_4$. Reaction of $WSeCl_4$ with ligands L gave $[WSeCl_4(L)]$ (L = MeCN, DMF, thf, py, $OPPh_3$, 2,2′-bipy, $SeMe_2$, Se^nBu_2), whilst the dimers $[(WSeCl_4)_2(\mu\text{-L–L})]$ were formed with L–L = $Ph_2P(O)CH_2P(O)Ph_2$, 1,4-dioxane and 4,4′-bipyridyl. The complexes were characterised by microanalysis, IR and ^{1}H NMR spectroscopy, and single crystal X-ray structures determined for $[WSeCl_4(L)]$ (L = $OPPh_3$, MeCN, DMF) and $[(WSeCl_4)_2(\mu\text{-L–L})]$ (L–L = 1,4-dioxane, 4,4′-bipyridyl). All except the 2,2′-bipy complex, which is probably seven-coordinate, contain six-coordinate tungsten with the neutral donor *trans* to W=Se. Alkylphosphines, including PMe_3 and PEt_3, decompose $WSeCl_4$ upon contact, forming phosphine selenides ($SePR_3$). In contrast, the selenoether complexes $[WSeCl_4(SeMe_2)]$ and $[WSeCl_4(Se^nBu_2)]$ were isolated and characterised. The crystal structure of the minor W(VI) by-product, $[(WSeCl_4)_2(\mu\text{-}SeMe_2)]$, was determined and using SMe_2, a few crystals of the W(V) species, $[\{WCl_3(SMe_2)\}_2(\mu\text{-Se})(\mu\text{-}Se_2)]$, were obtained and structurally characterised. The isolated W(VI) complexes are compared with those of $WOCl_4$ and $WSCl_4$ and the combination of experimental and computational data are consistent with $WSeCl_4$ being a weaker Lewis acid and its complexes significantly less stable than those of the lighter analogues, especially in solution. Low pressure chemical vapour deposition (LPCVD) using $[WSeCl_4(Se^nBu_2)]$ in the range 660–700 °C (0.1 mmHg) produced highly reflective thin films, which were identified to be WSe_2 by grazing incidence X-ray diffraction (XRD), scanning electron microscopy (SEM), X-ray photoelectron spectroscopy (XPS) and Raman spectroscopy. XRD analysis of the thinner films revealed them to be highly oriented in the <00*l*> direction.

Received 24th November 2021,
Accepted 7th January 2022

DOI: 10.1039/d1dt03980f

rsc.li/dalton

Introduction

Transition metal oxide halides have played a major role in the development of coordination and organometallic chemistry and in the applications of early d-block elements.[1–3] In contrast, the heavier analogues, the sulfide and selenide halides, are little known and have been much less studied.[4,5] There are no examples of molecular chalcogenide iodides, and whilst chalcogenide fluorides exist for Mo and W, their coordination chemistry is unexplored.[6] The synthesis and chemistry of MEX_3 (M = Nb, Ta; E = S, Se; X = Cl, Br) and WEX_4 were developed in the period 1965–1985, much of it by the groups of Fowles, Rice and Drew.[4,5] We have recently undertaken re-investigations and comparisons of the coordination chemistry

[a]*School of Chemistry, University of Southampton, Southampton SO17 1BJ, UK. E-mail: V.K.Greenacre@soton.ac.uk, G.Reid@soton.ac.uk*
[b]*School of Electronics and Computer Science, University of Southampton, Southampton SO17 1BJ, UK*

†Electronic supplementary information (ESI) available: Crystallographic parameters (Table S1), IR and NMR spectra for the new complexes (Fig. S2–S28), grazing incidence XRD patterns for further WSe_2 films obtained in this work (Fig. S29), together with computational data from DFT calculations (Tables S2–S5 and Fig. S30). CCDC 2122137 ($WSeCl_4$), 2122138 ($[WSeCl_4(OPPh_3)]$), 2122139 ($[WSeCl_4(DMF)]$), 2122140 ($[WSeCl_4(MeCN)]$), 2122141 ($[(WSeCl_4)_2(4,4'\text{-bipy})]$), 2122142 ($[WSeCl_4(dioxane)]$), 2122143 ($[(WSeCl_4)_2(\mu\text{-}SeMe_2)]$), 2122144 ($[(WSeCl_4)_2(\mu\text{-Se})(\mu\text{-}Se_2)]$). For ESI and crystallographic data in CIF or other electronic format see DOI: 10.1039/d1dt03980f

of $WSCl_4$ and $WSCl_3$ with those of $WOCl_4$ and $WOCl_3$ with a range of N- and O-donor ligands,[7] as well as with the softer phosphines and arsines,[8] and thioethers.[9] Comparisons of the chemistries of $TaOCl_3$ and $TaSCl_3$ have also been reported.[10,11] Thioether complexes of $NbSCl_3$, of type $[\{NbSCl_3(SR_2)\}_2]$ (R = Me, ^{n}Bu) are obtained from reaction of $NbCl_5$, SR_2 and $S(SiMe_3)_2$ in CH_2Cl_2, whilst $[NbSCl_3(L–L)]$ (L–L = MeS$(CH_2)_2$SMe, MeS$(CH_2)_3$SMe, ^{i}PrS$(CH_2)_2$S^{i}Pr and ^{n}BuS$(CH_2)_3$S^{n}Bu) are made from reaction of L–L with pre-formed $[NbSCl_3(MeCN)_2]$.[12] Selected examples can function as single source precursors for low pressure chemical vapour deposition (LPCVD) of thin films of 3R-NbS_2.[12] $[WSCl_4(SMe_2)]$ and $[(WSCl_4)_2\{\mu\text{-RS}(CH_2)_2\text{SR}\}]$ (R = Me, Ph, ^{i}Pr) and $[(WSCl_4)_2\{\mu\text{-MeS}(CH_2)_3\text{SMe}\}]$ have been made by direct reaction of $WSCl_4$ with the thioether in anhydrous CH_2Cl_2 solution.[9] We also showed that $[(WSCl_4)_2\{\mu\text{-}^i\text{PrS}(CH_2)_2\text{S}^i\text{Pr}\}]$ functions as a single source precursor to deposit 2H-WS_2 thin films by low pressure chemical vapour deposition (LPCVD),[9] providing further motivation to develop the chemistry of $WSeCl_4$ and its complexes.

Attempts to prepare dithio- or diseleno-ether complexes of $NbSeCl_3$ were unsuccessful, but reaction of $NbCl_5$, Se^{n}Bu$_2$ and $(Me_3Si)_2$Se in CH_2Cl_2 gave black $[NbSe_2Cl_3(Se^nBu_2)]$.[12] The structure of the latter is unknown, but may contain a diselenide unit ($[Se_2]^{2-}$). This compound deposits 2H-$NbSe_2$ films by LPCVD at 600–700 °C, 0.05 mmHg.[12]

The early transition metal dichalcogenides ME_2 (M = Nb, Ta, Mo, V, W, *etc.*, E = S, Se or Te) are layered semiconductors with good stabilities, and their properties can be tuned through the choice of metal and chalcogen.[13] This versatility gives rise to a plethora of applications in (opto)electronics, magnetic materials, spintronics, sensors and electrocatalysis, which are very active areas of research.[13–16] Production of the materials as thin films maximises the anisotropy of their magnetic or electronic properties, hence techniques to deposit 2D layers are of particular interest. Chemical vapour deposition (CVD) is widely used in industry as a low-cost, scalable and very versatile method to deposit such films using either dual or single source precursors.[13–19] The latter can offer better control of film stoichiometry, cost-effective use of reagents, as well as the ability to selectively deposit the metal chalcogenide film onto lithographically patterned substrates.[18] The application of molecular transition metal complexes as single source CVD precursors for the growth of metal chalcogenide thin films has been reviewed recently.[20]

Although $WSeCl_4$ was first described in 1974,[21] the few coordination complexes known are described in papers focussed rather on $WSCl_4$ adducts,[5,22–24] and a more detailed investigation of the selenide chloride is required to develop its chemistry and to determine if it could be the basis of a single source low pressure CVD route to WSe_2. A small number of dual source CVD routes to WSe_2 films have been described,[19,20] including using WCl_6 and $SeEt_2$ in atmospheric pressure CVD,[25] however, to the best of our knowledge there are no single source CVD reagents for tungsten diselenide films.

Here we report a detailed study of the synthesis, single crystal and powder X-ray structure and properties of $WSeCl_4$, its coordination chemistry with a range of neutral N-, O- and Se-donor ligands, and demonstrate that the new complex, $[WSeCl_4(Se^nBu_2)]$, can function as a single source precursor for the CVD growth of continuously interconnected WSe_2 thin films.

Results and discussion

$WSeCl_4$

$WSeCl_4$ was prepared by heating together a finely ground mixture of WCl_6 and Sb_2Se_3 in a 3 : 1 molar ratio *in vacuo*, according to the general method of Britnell *et al.*[21] Obtaining good yields of the pure product required very careful control of the conditions, and hence the preparation and apparatus used in this work are described in detail in the Experimental section. The green powdered $WSeCl_4$ is moisture sensitive, but can be stored in a sealed container in the glove box indefinitely. Attempts to obtain $WSeCl_4$ by reaction of WCl_6 and Se$(SiMe_3)_2$ in a variety of organic solvents, including CH_2Cl_2, toluene or MeCN, and at various temperatures from ambient to −78 °C, failed. This contrasts with the ready synthesis of $WSCl_4$ from WCl_6 and $S(SiMe_3)_2$, and $WOCl_4$ from WCl_6 and $O(SiMe_3)_2$.[7–9,26] Refluxing $WSeCl_4$ with $Cl_2C{=}CCl_2$ also failed to produce $WSeCl_3$, whereas the similar reaction of $WSCl_4$ and $Cl_2C{=}CCl_2$ forms $WSCl_3$.[27]

Green single crystals of $WSeCl_4$, which were obtained during the synthesis by sublimation, contained two independent molecules in the asymmetric unit, both monomeric square pyramids, with similar bond lengths and angles (Fig. 1). In contrast, $WSCl_4$ adopts two structurally distinct

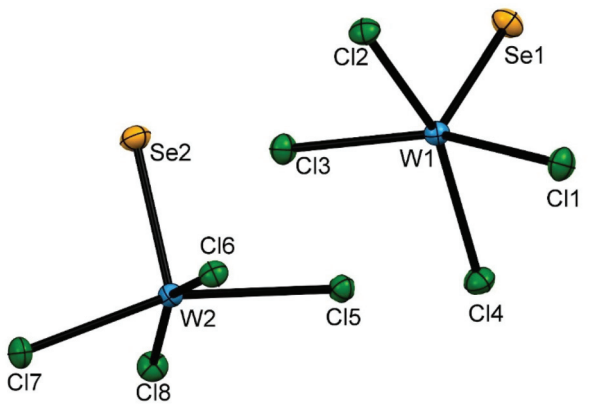

Fig. 1 The crystal structure of the two independent molecules of $WSeCl_4$ in the asymmetric unit showing the atom numbering scheme and with the ellipsoids drawn at the 50% probability level. Selected bond lengths (Å) and angles (°) are: W1–Se1 = 2.2099(4), W1–Cl3 = 2.2944(9), W1–Cl2 = 2.3048(8), W1–Cl4 = 2.3045(8), W1–Cl1 = 2.3038(9), Se1–W1–Cl3 = 101.46(2), Se1–W1–Cl2 = 101.15(2), Se1–W1–Cl4 = 101.98(2), Se1–W1–Cl1 = 101.66(3), Cl3–W1–Cl2 = 87.74(3), Cl3–W1–Cl4 = 87.68(3), Cl1–W1–Cl2 = 88.06(3), Cl1–W1–Cl4 = 87.30(3), W2–Se2 = 2.2128(4), W2–Cl5 = 2.3419(8), W2–Cl7 = 2.2762(9), W2–Cl6 = 2.3949(8), W2–Cl8 = 2.2689(8), Se2–W2–Cl5 = 98.24(2), Se2–W2–Cl7 = 101.18(2), Se2–W2–Cl6 = 97.65(2), Se2–W2–Cl8 = 101.49(2), Cl5–W2–Cl6 = 85.15(3), Cl7–W2–Cl6 = 88.32(3), Cl8–W2–Cl5 = 88.58(3), Cl8–W2–Cl7 = 91.45(3).

polymorphs, a dimer, $[SCl_3W(\mu\text{-}Cl)_2WCl_3S]$,[28] and a tetramer, $[Cl_4SW(\mu\text{-}Cl)SCl_2W(\mu\text{-}Cl)_2WCl_2S(\mu\text{-}Cl)WSCl_4]$.[29] $WSCl_4$ monomers are present in $WSCl_4{\cdot}S_8$, which seems to be best described as co-crystallised $WSCl_4$ and cyclo-octasulfur, rather than an adduct.[30]

Powder X-ray diffraction (PXRD) data from the powdered bulk $WSeCl_4$ (ESI Fig. S1†) shows the same polymorph as identified in the single crystal structure, with no evidence for a second form. This solid state structure is very similar to that reported for the compound from vapour phase electron diffraction.[31]

The IR spectrum of $WSeCl_4$ (Nujol mull) shows (ESI. Fig. S2†) a medium feature at 387 cm^{-1} assigned as ν(W═Se) and intense features at 353 and 367 cm^{-1} assigned as ν(W–Cl). The ν(W═Se) is in good agreement with literature data, *viz.* ν(W═Se) 388,[31] or 396 cm^{-1},[21] and is supported by DFT calculations (below). The IR spectrum of $WSeCl_4$ vapour, isolated in a N_2 matrix at 10 K showed vibrations at 399 and 369 cm^{-1}, both tentatively assigned as ν(W–Cl), while ν(W═Se) was not identified.[32] The reassignment of the band at 399 cm^{-1} as ν(W═Se) seems merited in the light of these new results.

Density functional theory (DFT) calculations

To further explore the structure of $WSeCl_4$, to investigate the frontier orbitals and to complement the experimental data with IR spectroscopic assignments, the ground state geometry of $WSeCl_4$ was optimised using DFT methods, starting from the solid-state structure. These calculations were carried out with the B3LYP-D3 functional,[33] (lanl2dz on W; 6-311G(d) on Se and Cl atoms) and the geometrical parameters were found to be in good agreement with the solid-state values (Fig. 2 and ESI Table S2†). The predicted IR harmonic wavenumbers in Table 1 confirm the assignment of the ν(W═Se) peak in the experimental IR spectrum at a slightly higher frequency than ν(W–Cl).

As discussed above, the known polymorphs of $WSCl_4$ in the solid state are a dimer or tetramer, while the crystals obtained of $WSeCl_4$ show this to be a monomer. To further explore this difference, DFT calculations were undertaken to compare the energy of formation of the optimised selenide and sulfide dimer (with bridging Cl), *i.e.* the energy difference upon going from 2 $WECl_4$ to $[ECl_3(W(\mu\text{-}Cl)_2WCl_3E]$. This showed the energy of formation of the sulfide-bridged dimer (ΔE) to be more negative (−78.4 kJ mol^{-1}) than the selenide bridged dimer (−76.3 kJ mol^{-1}), supporting the conclusion that for $WSCl_4$ the dimer is more stable. This is further evidenced by examining the molecular orbitals of $WSCl_4$ and $WSeCl_4$ (ESI Fig. S30†), particularly the HOMO and HOMO−1 orbitals, which show more extensive contribution from the chlorides in $WSCl_4$ compared to the $WSeCl_4$.

Table 1 Selected experimental and calculated IR stretching and bending vibrations

Bond	Experimental/ cm^{-1}	DFT (B3LYP-D3) Adjusted[a] wavenumber/ cm^{-1}	Intensity/km mol^{-1}
W═Se	388	370	25
W–Cl	367		
W–Cl	353	354	6
W–Cl	336	333	119

[a] Scaling factor used 0.966 (ref. 34).

Finally, calculations were undertaken to explore the relative Lewis acidities of the $WECl_4$ species (E = S, Se) by considering the following reaction:

$$WECl_4 + OPPh_3 \rightarrow WECl_4(OPPh_3)\ (E = S, Se);$$

where $\Delta E = E([WSCl_4(OPPh_3)]) - E(OPPh_3) - E(WSCl_4)$.

These showed that the ΔE for E = S (−161.2 kJ mol^{-1}) was slightly more negative than for E = Se (−156.5 kJ mol^{-1}), consistent with $WSCl_4$ being the more Lewis acidic of the pair.

Complexes with N- and O-donor ligands

Despite the lower Lewis acidity of $WSeCl_4$, the syntheses of a range of its complexes with neutral Group 15 and 16 donor ligands was undertaken (Scheme 1), and their properties compared with those of the $WOCl_4$ and $WSCl_4$ analogues. The reactions with ligands occurred readily, although the products were often unstable in solution and sometimes also in the solid state. Successful syntheses used carefully chosen (low polarity, weakly-coordinating, volatile) solvents and required

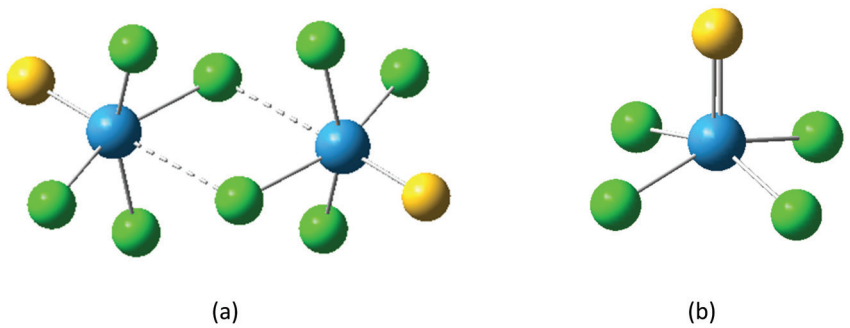

Fig. 2 Schematic showing the DFT calculated structures for (a) $WECl_4$ and (b) $[ECl_3W(\mu\text{-}Cl)_2WCl_3E]$ (E = S, Se).

rapid isolation of the products. Attempted recrystallisation of the complexes often resulted in significant decomposition rather than purification. The solution spectra also needed to be recorded from freshly prepared solutions to minimise significant decomposition.

The reaction of $WSeCl_4$ with one molar equivalent of DMF, thf, pyridine, $OPPh_3$ and 2,2′-bipy, as described in the Experimental section, resulted in green powders $[WSeCl_4(L)]$; often the choice of solvent was key to obtaining the target complex in a pure form. In contrast, $[WSeCl_4(MeCN)]$ could be obtained from a range of solvents, as well as from neat MeCN, and could be used as a synthon for other complexes, although it proved to be little different from using $WSeCl_4$ itself in most cases. The bidentates, $Ph_2P(O)CH_2P(O)Ph_2$ ($dppmO_2$), 1,4-dioxane and 4,4′-bipyridyl (L–L), reacted with two equivalents of $WSeCl_4$ to form the ligand-bridged dimers, $[(WSeCl_4)_2(\mu\text{-L–L})]$. With one exception, ($[WSeCl_4(2,2'\text{-bipy})]$ below), the spectroscopic data show the complexes contain six-coordinate distorted octahedral tungsten environments, which was confirmed by X-ray crystal structures of five examples (Fig. 3–7), showing the neutral ligand occupying the vacant site *trans* to W═Se in $WSeCl_4$. As is found in other complexes of this type, the tungsten lies out of the Cl_4 plane towards the selenium. The effect of coordination on the W═Se and W–Cl bond lengths is small, with only slightly longer bonds in the six-coordinate complexes. The ^{1}H and (where appropriate) $^{31}P\{^1H\}$ NMR spectra confirm the presence of the coordinated neutral ligand, with chemical shifts generally very similar to those in the $WOCl_4$ and $WSCl_4$ analogues.[7] The poor solubility and solution instability generally precluded using ^{77}Se NMR spectroscopy (^{77}Se: 7.58%, $I = \frac{1}{2}$, Ξ = 19.09 MHz, D_c = 2.98) for their characterisation.

In the IR spectra, the ν(W–Cl) occurred as two strong overlapping bands in the region 350–310 cm^{-1} and ν(W═Se) as a weak or medium intensity band in the range 380–350 cm^{-1}, somewhat lower frequency than in $WSeCl_4$ itself, in accord with the increase in the coordination number.

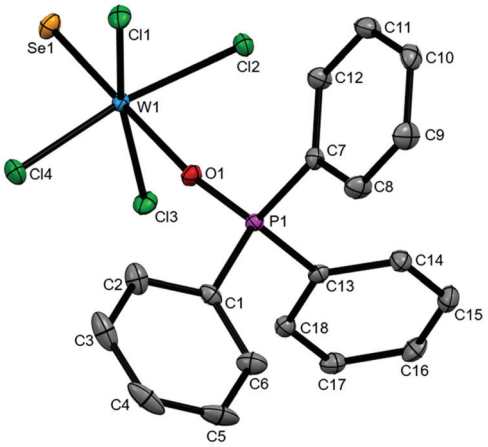

Fig. 3 The structure of $[WSeCl_4(OPPh_3)]$ showing the atom numbering scheme and ellipsoids are shown at the 50% probability level. H atoms are omitted for clarity. Selected bond lengths (Å) and angles (°) are: W1–Se1 = 2.2321(2), W1–Cl1 = 2.3514(5), W1–Cl2 = 2.3577(5), W1–Cl3 = 2.3217(5), W1–Cl4 = 2.3218(5), W1–O1 = 2.1669(14), P1–O1 = 1.5066(15), Se1–W1–Cl1 = 97.836(15), Se1–W1–Cl2 = 94.628(14), Se1–W1–Cl3 = 96.375(15), Se1–W1–Cl4 = 97.047(15), Cl1–W1–Cl2 = 87.552(17), Cl3–W1–Cl2 = 88.861(18), Cl3–W1–Cl4 = 91.204(19), Cl4–W1–Cl1 = 89.494(18), O1–W1–Cl1 = 82.53(4), O1–W1–Cl2 = 84.52(4), O1–W1–Cl3 = 83.23(4), O1–W1–Cl4 = 83.81(4), P1–O1–W1 = 167.82(10).

Once isolated, the $[WSeCl_4(2,2'\text{-bipy})]$ proved to very poorly soluble in suitable solvents, and X-ray quality crystals could not be obtained. However, the ^{1}H NMR spectrum showed equivalent pyridyl rings, whilst the ν(W–Cl) = 318, 304 cm^{-1} and ν(W═Se) = 345 cm^{-1} are lower than in the six-coordinate complexes, providing supporting evidence that $[WSeCl_4(2,2'\text{-bipy})]$ is probably seven-coordinate and pentagonal bipyramidal. The corresponding $[WOF_4(2,2'\text{-bipy})]$, $[WOCl_4(2,2'\text{-bipy})]$ and $[WSCl_4(2,2'\text{-bipy})]$ are also thought to be seven-coordinate based upon spectroscopic data, and $[WOF_4\{o\text{-}C_6H_4(PMe_2)_2\}]$, $[WOCl_4\{o\text{-}C_6H_4(AsMe_2)_2\}]$ and $[WSCl_4\{o\text{-}C_6H_4(PMe_2)_2\}]$ have

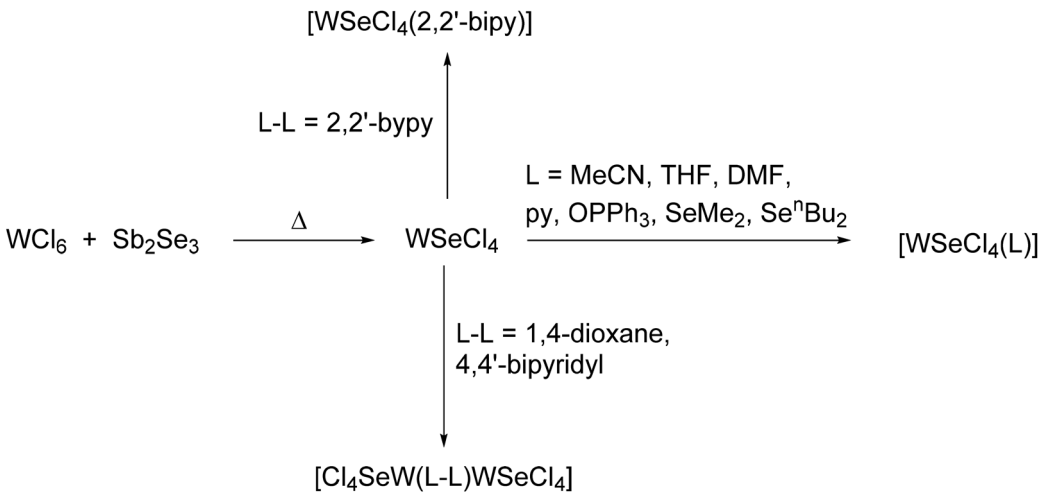

Scheme 1 Synthesis routes to $WSeCl_4$ and its complexes.

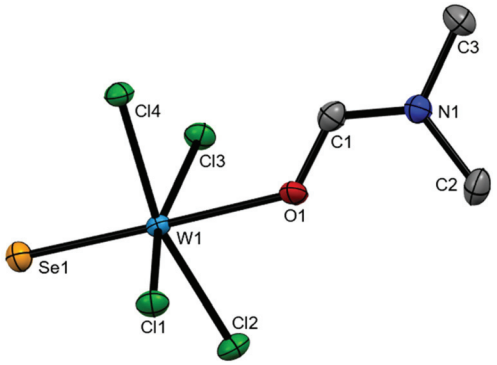

Fig. 4 The structure of [WSeCl$_4$(DMF)] showing the atom numbering scheme and ellipsoids are shown at the 50% probability level. H atoms and a C_6H_6 solvent molecule are omitted for clarity. Note that the disorder in the structure was modelled using split atom occupancies and only the major form is shown here. Selected bond lengths (Å) and angles (°) are: W1–Se1 = 2.2478(7), W1–Cl1 = 2.3283(15), W1–Cl2 = 2.3252(15), W1–Cl3 = 2.3422(14), W1–Cl4 = 2.3466(14), W1–O1 = 2.173(4), Se1–W1–Cl1 = 98.79(4), Se1–W1–Cl2 = 98.22(4), Se1–W1–Cl3 = 95.60(4), Se1–W1–Cl4 = 96.22(4), Cl1–W1–Cl4 = 88.69(5), Cl2–W1–Cl1 = 89.50(6), Cl2–W1–Cl3 = 89.44(6), Cl3–W1–Cl4 = 88.75(5), O1–W1–Cl1 = 83.06(12), O1–W1–Cl2 = 81.74(13), O1–W1–Cl3 = 82.55(12), O1–W1–Cl4 = 83.82(13).

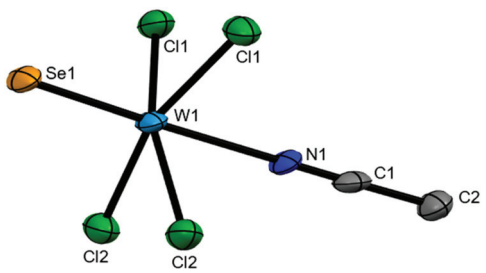

Fig. 5 The structure of [WSeCl$_4$(MeCN)] showing the atom numbering scheme. Ellipsoids are shown at the 50% probability level and H atoms are omitted for clarity. Selected bond lengths (Å) and angles (°) are W1–Se1 = 2.2312(9), W1–Cl1 = 2.3248(17), W1–Cl2 = 2.3208(17), W1–N1 = 2.330(7), Se1–W1–Cl1 = 97.83(4), Se1–W1–Cl2 = 99.32(4), Cl1–W1–Cl1 = 90.30(9), Cl1–W1–N1 = 81.05(13), Cl2–W1–Cl1 = 88.83(6), Cl2–W1–Cl2 = 86.95(9), Cl2–W1–N1 = 81.83(14).

been established as pentagonal bipyramids by single crystal X-ray analysis.[8,35] Rather surprisingly, attempts to isolate the (unknown) anion, $[WSeCl_5]^-$ with a range of cations, including $[PPh_4]^+$ and $[NEt_4]^+$, have been unsuccessful thus far, whereas the $[WSCl_5]^-$ and $[WS_2Cl_4]^{2-}$ ions are well known.[36,37]

Reactions with soft P- and Se-donor ligands

The addition of PMe_3 or PEt_3 to a solution of $WSeCl_4$ in CH_2Cl_2 immediately produced orange-brown solutions in which the only species evident in the $^{31}P\{^1H\}$ NMR spectra, in addition to small amounts of the free phosphine, were the corresponding phosphine selenides $SePMe_3$ (δ_P = +9.4)[38] and $SePEt_3$ (δ_P = +45.2, $^1J_{PSe}$ = 680 Hz).[39] The reaction of $WECl_4$ (E = O, S, Se) with a large excess of PPh_3 over several days in toluene was reported to form $[WCl_4(PPh_3)_2]$ and $EPPh_3$.[40] Similar, but much faster abstraction of the selenium occurs on contact with alkyl phosphines. Similarly, reaction of o-$C_6H_4(PMe_2)_2$ with $WSeCl_4$ in CH_2Cl_2 instantly produced a green solution and a brown precipitate, and the $^{31}P\{^1H\}$ NMR spectrum showed several species present in the solution, with the major resonances at δ = +20 and +33, which may be due to phosphine selenides. This contrasts with the reactions of o-$C_6H_4(PMe_2)_2$ with $WOCl_4$ and $WSCl_4$, which gave high yields of the seven-coordinate complexes $[WECl_4\{o\text{-}C_6H_4(PMe_2)_2\}]$ (E = O, S), both of which were characterised, including the X-ray structure of the latter (as noted earlier).[8] Decomposition of $[WECl_4\{o\text{-}C_6H_4(PMe_2)_2\}]$ in CH_2Cl_2 solution over a few days gave crystals of a number of tungsten(v) species including $[WOCl_3\{o\text{-}C_6H_4(PMe_2)_2\}]$ and $[WCl_4\{o\text{-}C_6H_4(PMe_2)_2\}_2]^+$.[8] This contrasts with the immediate reduction of the metal in the $WSeCl_4$ systems in the present study. A few crystals obtained from the mother liquor of the o-$C_6H_4(PMe_2)_2$/$WSeCl_4$ reaction were identified by X-ray analysis as $[WCl_4\{o\text{-}C_6H_4(PMe_2)_2\}_2]Cl$; the same eight-coordinate cation was found among the decomposition products of $[WSCl_4\{o\text{-}C_6H_4(PMe_2)_2\}]$ in CH_2Cl_2.[8]

The reaction of $WSeCl_4$ with $SeMe_2$ in benzene resulted in green $[WSeCl_4(SeMe_2)]$, identified by microanalysis and its IR spectrum, which showed ν(W=Se) at 387 cm^{-1} and ν(W–Cl) at 343 cm^{-1}. Use of Se^nBu_2 in this reaction gave a dark red oil identified as $[WSeCl_4(Se^nBu_2)]$ from its IR, ^1H and $^{77}Se\{^1H\}$ NMR spectra, but attempts to isolate complexes with diselenoethers such as $[(WSeCl_4)_2\{\mu\text{-}RSe(CH_2)_2SeR\}]$ were unsuccessful. Similarly, attempts to prepare $[(WSCl_4)_2\{\mu\text{-}MeSe(CH_2)_2SeMe\}]$ were unsuccessful, although the $[WSCl_4(SeMe_2)]$ analogue is well characterised.[9] A few dark green crystals isolated from a solution of the $[WSeCl_4(SeMe_2)]$ monomer in C_6D_6 unexpectedly proved to be the dinuclear $[(WSeCl_4)_2(\mu\text{-}SeMe_2)]$ (Fig. 8), which shows two square pyramidal $WSeCl_4$ groups linked by a bridging $SeMe_2$ ligand. The d(W=Se) and d(W–Cl) are similar to those in the complexes with hard donor ligands (above), while the d(W–Se_{Me2}) is long at ~3.0 Å. Selenoethers bridging between two metal centres and formally using both lone pairs are known for many d-block metals,[41] although it was unexpected here given the modest acceptor ability of $WSeCl_4$. This dimer presumably crystallised as the least soluble species in a partially dissociated solution of $[WSeCl_4(SeMe_2)]$.

Similar reaction of $WSeCl_4$ with SMe_2 did not yield a pure product, however, a few crystals obtained by slow evaporation of CH_2Cl_2 from the reaction mixture were shown by X-ray crystallographic analysis to contain the W(v) dimer, $[\{WCl_3(SMe_2)\}_2(\mu\text{-}Se)(\mu\text{-}Se_2)]$ (Fig. 9). Previous work showed that decomposition of several $WSCl_4$ thioether complexes (or reduction with excess thioether) affords the corresponding W(v) complexes.[5,9] However, decomposition of the $WSeCl_4$ complexes prepared in the present study typically produced dark intractable solids, that were insoluble in organic solvents and could not be identified. Structurally characterised niobium(iv) complexes similar to $[Cl_3(SMe_2)W(\mu\text{-}Se)(\mu\text{-}Se_2)WCl_3(SMe_2)]$ include $[(tht)Br_2Nb(\mu\text{-}Se)(\mu\text{-}$

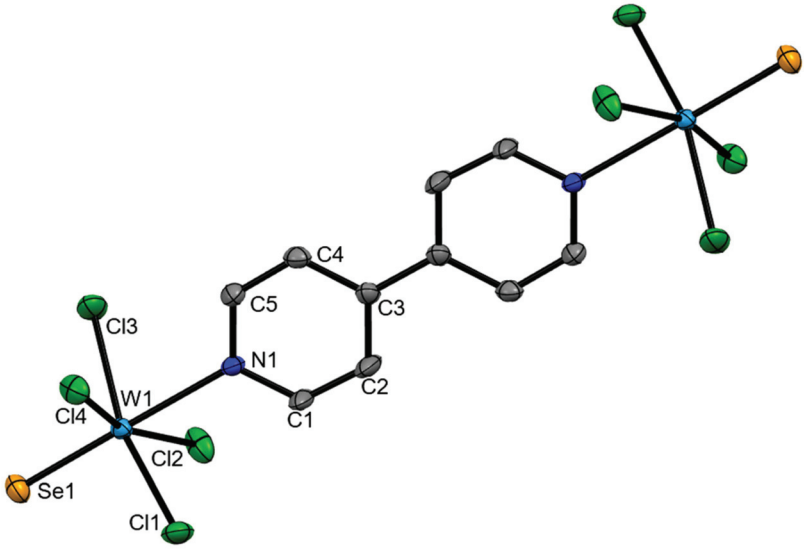

Fig. 6 The structure of [(WSeCl$_4$)$_2$(μ-4,4′-bipy)] showing the atom numbering scheme. Ellipsoids are shown at the 50% probability level and H atoms and benzene solvent molecules are omitted for clarity. The asymmetric unit consists of two of these molecules, only one of which is shown. Selected bond lengths (Å) and angles (°) are: W1–Se1 = 2.2424(7), W1–Cl4 = 2.3292(17), W1–Cl1 = 2.3150(16), W1–Cl3 = 2.3113(17), W1–Cl2 = 2.3214(18), W1–N1 = 2.391(5), Se1–W1–Cl4 = 97.47(4), Se1–W1–Cl1 = 98.68(5), Se1–W1–Cl3 = 98.66(5), Se1–W1–Cl2 = 98.08(5), Cl4–W1–N1 = 81.40(14), Cl1–W1–Cl4 = 88.40(6), Cl1–W1–Cl2 = 88.92(7), Cl1–W1–N1 = 81.42(13), Cl3–W1–Cl4 = 88.66(7), Cl3–W1–Cl2 = 89.34(7), Cl3–W1–N1 = 81.22(13), Cl2–W1–N1 = 83.05(14).

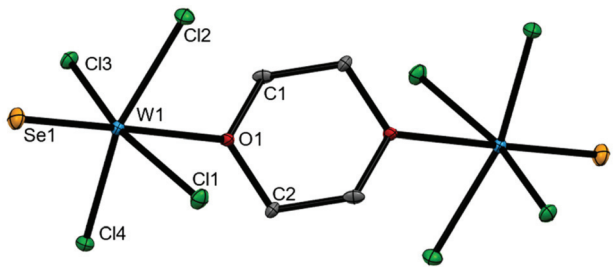

Fig. 7 The structure of [{WSeCl$_4$}$_2$(1,4-dioxane)] showing the atom numbering scheme. Ellipsoids are shown at the 50% probability level and H atoms are omitted for clarity. Selected bond lengths (Å) and angles (°) are: W1–Se1 = 2.2285(4), W1–Cl1 = 2.3138(8), W1–Cl2 = 2.3273(8), W1–Cl3 = 2.3069(8), W1–Cl4 = 2.3081(8), W1–O1 = 2.398(2), Se1–W1–Cl1 = 98.44(2), Se1–W1–Cl2 = 98.97(2), Se1–W1–Cl3 = 99.60(2), Se1–W1–Cl4 = 98.73(2), Cl1–W1–Cl2 = 88.20(3), Cl1–W1–O1 = 80.83(6), Cl2–W1–O1 = 81.40(6), Cl3–W1–Cl2 = 88.80(3), Cl3–W1–Cl4 = 89.51(3), Cl3–W1–O1 = 81.12(6), Cl4–W1–Cl1 = 87.95(3), Cl4–W1–O1 = 80.88(6).

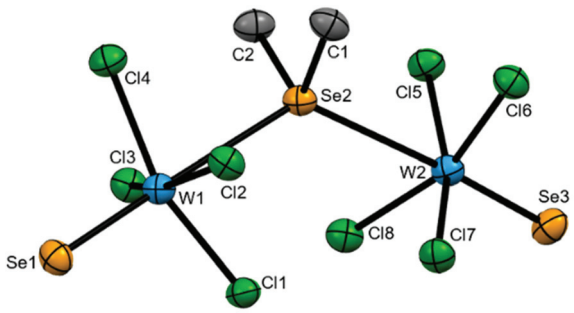

Fig. 8 The structure of [(WSeCl$_4$)$_2$(μ-SeMe$_2$)] showing the atom numbering scheme. Ellipsoids are shown at the 50% probability level and H atoms are omitted for clarity. Selected bond lengths (Å) and angles (°) are W1–Se1 = 2.2374(8), W2–Se3 = 2.2255(9), W1–Se2 = 3.0107(8), W2–Se2 = 3.0814(8), W1–Cl = 2.2871(19)–2.3311(19), W2–Cl = 2.3006(18)–2.3130(18), Se1–W1–Se2 = 178.42(3), Se3–W2–Se2 = 176.28(3), W1–Se2–W2 = 127.82(3), Se1–W1–Cl = 98.42(5) – 100.95(5), Se2–W1–Cl = 80.03(5) – 81.91(5), Se3–W2–Cl = 98.86(6) – 101.89(6), Se2–W2–Cl = 76.67(5) – 81.78(5).

Se$_2$)NbBr$_2$(tht)] (tht = tetrahydrothiophene) and [(SMe$_2$)Cl$_2$Nb(μ-Se$_2$)$_2$NbCl$_2$(SMe$_2$)].[5,21,42,43] In fact, very little is known about WSeCl$_3$ and no complexes with neutral ligands have been described.[5]

Growth of WSe$_2$ thin films *via* low pressure CVD

The isolation of [WSeCl$_4$(Se^{n}Bu$_2$)] as an oil, containing a 1 : 2 ratio of tungsten to selenium, and with the *n*-butyl groups on the selenoether providing a potential low energy thermal decomposition pathway (*e.g. via* β-hydride elimination), raised the prospect that this might serve as a single source CVD precursor for the growth of tungsten diselenide thin films onto fused silica substrates, in a similar manner to [(WSCl$_4$)$_2$\{μ-^{i}PrS(CH$_2$)$_2$S^{i}Pr\}], which deposits WS$_2$ films.[9] LPCVD using [WSeCl$_4$(Se^{n}Bu$_2$)] produced highly reflective, silvery films of WSe$_2$ at 0.1 mmHg and 660–700 °C.

Grazing incidence XRD analysis of the films obtained from [WSeCl$_4$(Se^{n}Bu$_2$)] (Fig. 10 and S29†) are consistent with polycrystalline 4H WSe$_2$ in space group $P6_3/mmc$. Lattice parameters were refined as: a = 3.2829(11), c = 13.130(6) (R_{wp} = 7.82%, literature: a = 3.285(1); c = 12.961(1) Å from the XRD

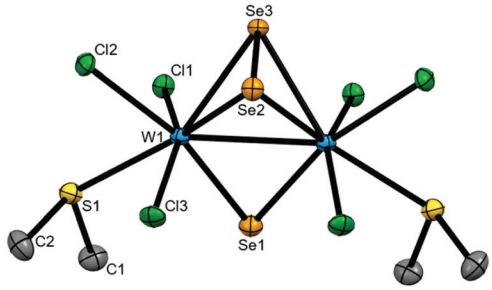

Fig. 9 The structure of $[\{WCl_3(SMe_2)\}_2(\mu\text{-}Se)(\mu\text{-}Se_2)]$ showing the atom numbering scheme. Ellipsoids are shown at the 50% probability level and H atoms are omitted for clarity. Selected bond lengths (Å) and angles (°): W1–W1 = 2.8021(6), W1–Se1 = 2.4310(9), W1–Se2 = 2.5687(9), W1–Se3 = 2.5589(9), Se2–Se3 = 2.2633(14), W1–Cl1 = 2.4259(16), W1–Cl2 = 2.3944(16), W1–Cl3 = 2.3791(16), W1–S1 = 2.6017(18), W1–Se1–W1 = 70.39(3), W1–Se2–W1 = 66.11(3), W1–Se3–W1 = 66.40(3), Cl1–W1–S1 = 71.16(6), Cl2–W1–S1 = 76.35(6), Cl3–W1–S1 = 82.26(6), Cl3–W1–Cl1 = 153.31(6), Cl3–W1–Cl2 = 88.76(6), Cl2–W1–Cl1 = 87.33(6).

pattern in Fig. S29a†).[44] The grazing incidence diffraction patterns of the thinner films, for example, Fig. 10, are almost completely dominated by the 002 reflection, consistent with significant preferred orientation in the <00*l*> direction. This orientation is not unusual, as these layered materials typically grow initially with the *c* axis normal to the substrate, and suggests that the majority of the platelet crystals have grown in that orientation, with the platelets flat to the substrate. The average crystallite size in the WSe_2 film was determined to be 9.4(14) nm based on the grazing incidence XRD data in Fig. S29a,† using the Williamson-Hall method.

Fig. 11 presents top-view SEM images of the as-deposited WSe_2 thin film. The film displays a smooth underlying interconnected polycrystalline layer with some more randomly oriented crystallites on top. The underlying layer comprises of hexagonal plate-like crystallites oriented with the *c*-axis normal to the substrate. This is supported by the preferential growth observed in the XRD patterns in Fig. 10 and Fig. S29b.†

The Raman spectrum for the WSe_2 film deposited *via* LPCVD is presented in Fig. 12. The two significant peaks located at 248.7 cm^{-1} and 258.5 cm^{-1} are commonly known as the $E_{2g}{}^1$ (green) and A_{1g} (orange) vibrational modes, respectively, and are in good agreement with current literature.[45] The inset is a schematic of the $E_{2g}{}^1$ and the A_{1g} modes, which represent the in-plane and out-of-plane vibrational modes, respectively.[46] The relative intensities of the $E_{2g}{}^1$ and the A_{1g} modes suggest the suppression of the out-of-plane A_{1g} mode being due to the thin nature of the film.[46,47] The peaks labelled 2M are likely to be related to the combinational second order Raman modes.[46–48] The origin of peak *x* located at 307.3 cm^{-1} is likely to be a combinational mode of low frequency modes due to its relatively large frequency. It has been suggested that this peak is linked to coupling of the $E_{2g}{}^1$ mode and an intra-layer shear force, due to reports that suggest suppression of this peak in monolayered samples.[46,49,50]

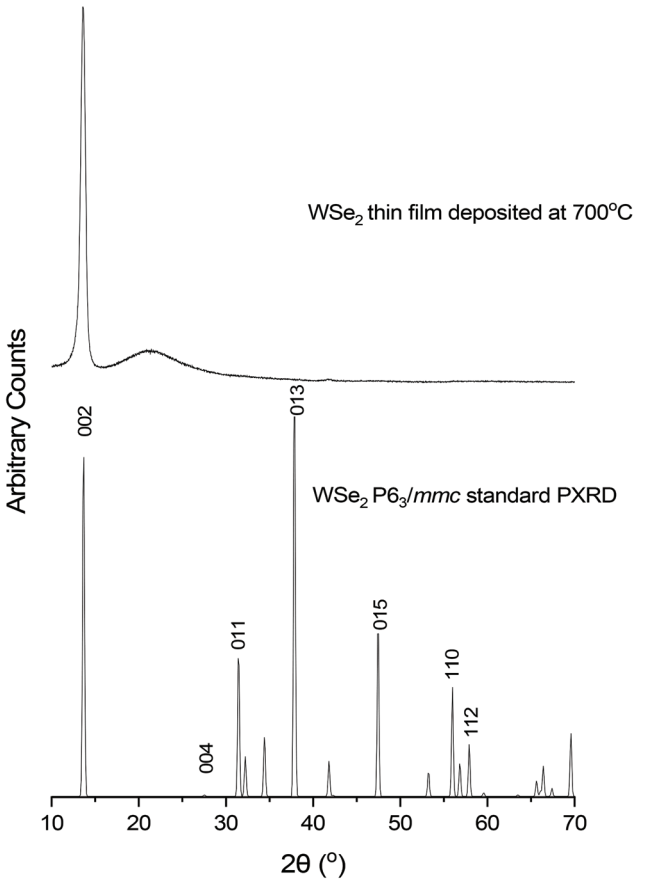

Fig. 10 Grazing incidence XRD pattern (top) from a WSe_2 thin film deposited by low pressure CVD using $[WSeCl_4(Se^nBu_2)]$. The broad feature at 2θ = 20–25° is from the SiO_2 substrate. XRD pattern for bulk WSe_2 (bottom).[44]

The film composition was investigated by X-ray photoelectron spectroscopy (XPS). Fig. 13a presents the XPS survey spectrum of the film. Both the W and Se peaks are clearly presented, with no impurities (*e.g.* C, Cl) observed, suggesting the WSe_2 film is of high quality. Elemental scans were conducted of both the W 4f and Se 3d orbitals (shown in Fig. 13b–c). From the elemental scan of the W 4f orbital, two significant peaks positioned at 32.2 eV and 34.3 eV were observed. These peaks are in good agreement with literature and represent electron emission from the $4f_{7/2}$ and $4f_{5/2}$ atomic orbitals.[51] An additional peak located at 37.5 eV was noted in the W scan, which has been suggested to be related to W $5p_{3/2}$.[52] The Se scan in Fig. 13 displays two significant peaks at 54.6 eV and 55.7 eV related to the $3d_{5/2}$ and $3d_{3/2}$ orbitals respectively.[52] From the spectra shown in Fig. 13, a $WSe_{2.1}$ composition for the deposited films has been derived (*i.e.* W : Se = 32.1% : 67.9%).

Experimental

Syntheses were performed using standard Schlenk and glovebox techniques under a dry N_2 atmosphere. Solvents and

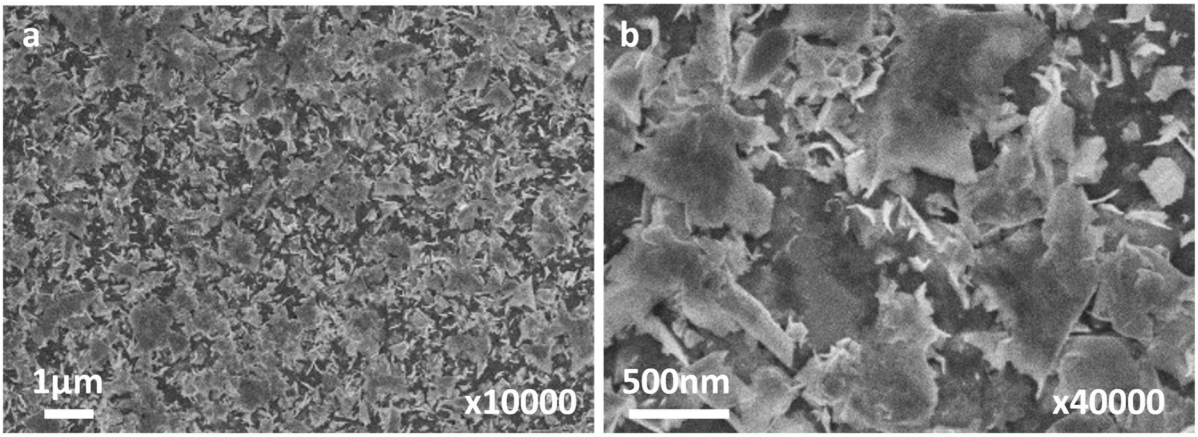

Fig. 11 Morphological characterisation *via* SEM imaging for an as-deposited WSe_2 film produced *via* low pressure CVD using [$WSeCl_4(Se^nBu_2)$], taken at magnifications (a) ×10 000 and (b) ×40 000.

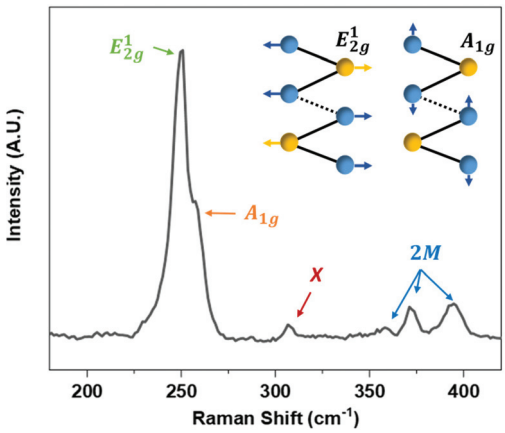

Fig. 12 Raman spectrum of the WSe_2 film obtained using [$WSeCl_4(Se^nBu_2)$].

ligands were dried by distillation from CaH_2 (CH_2Cl_2, MeCN, DMF,) or Na/benzophenone ketyl (toluene, *n*-hexane, diethyl ether, thf, 1,4-dioxane, py). WCl_6, PMe_3, PEt_3, SMe_2, $SeMe_2$, 2,2′-bipy and 4,4′-bipy were obtained from Sigma-Aldrich. $Ph_2P(O)CH_2P(O)Ph_2$ was obtained by air oxidation of the corresponding diphosphine in CH_2Cl_2, catalysed by SnI_4.[52] Solid ligands were dried *in vacuo* for several hours immediately before use.

Infrared spectra were recorded on a PerkinElmer Spectrum 100 spectrometer in the range 4000–200 cm^{-1}, with samples prepared as Nujol mulls between CsI plates. ^{1}H and ^{31}P{^{1}H} NMR spectra were recorded using a Bruker AV 400 spectrometer and referenced to the residual protio-resonance of the solvent and 85% H_3PO_4. Microanalyses on new compounds were undertaken by London Metropolitan University or Medac Ltd. Note that the complexes were generally very unstable, readily decomposing within a few hours in some cases. This hindered attempts to obtain satisfactory microanalyses on some samples from outsourced measurements – as noted below.

X-ray experimental

Crystals were grown from slow evaporation of saturated solutions in CH_2Cl_2 or by liquid–liquid diffusion using CH_2Cl_2 and hexane. Data collections used either a Rigaku OD UG2 goniometer equipped with a HyPix 6000HE hybrid pixel array detector mounted at the window of an FR-E + SuperBright molybdenum (λ = 0.71073 Å) rotating anode generator with VHF Varimax optics (70 micron focus) with the crystal held at 100 K (N_2 cryostream), or a Rigaku OD UG2 goniometer equipped with a HyPix 6000HE hybrid pixel array detector mounted at the window of a MicroMax 007HF copper (λ = 1.54184 Å) rotating anode generator with VHF Varimax optics (70 micron focus) with the crystal held at 100 K (N_2 cryostream). Crystallographic parameters are presented in Table S1.† Structure solution and refinement were performed using SHELX(T)-2018/2, SHELX-2018/3 through Olex2[53] and were mostly straightforward. H atoms were added and refined with a riding model. Where additional restraints were required, details are provided in the cif file for each structure found on CCDC.†

Computational experimental

Geometry optimisation and frequency calculations were performed on $WSeCl_4$ with the B3LYP hybrid functional, with the Grimme correction for dispersion (D3(BJ)),[33] using Gaussian 16.[54] A 6-311G(d) basis set was used on Se and Cl atoms while the RECP basis set LANL2DZ was used on the W atom. Calculations on $WSCl_4$ were based on the crystal structure for $WSeCl_4$, while the starting geometries for the dimers ([$ECl_3W(\mu\text{-}Cl)_2WCl_3E$]) (E = S, Se) were based on the structure for E = S reported in the literature.[28]

For the complexes, the starting geometries for [$WSeCl_4(OPPh_3)$] and [$WSCl_4(OPPh_3)$][9] came from their respective crystal structures with the same functional and

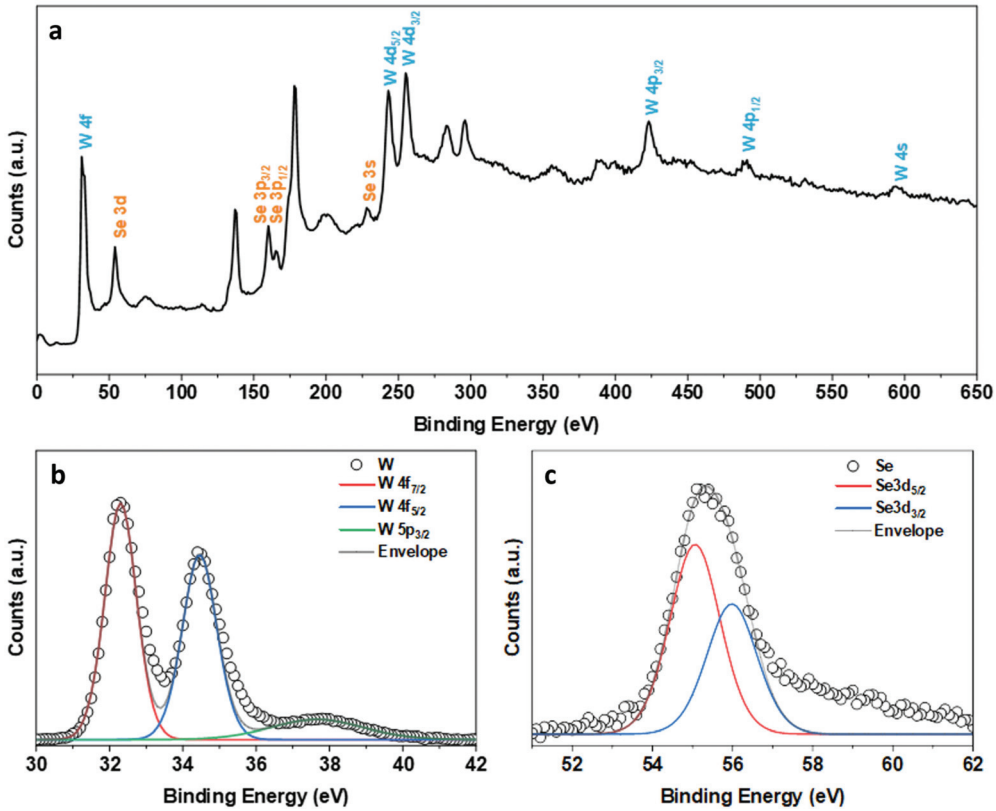

Fig. 13 XPS characterisation of an as-deposited WSe_2 film produced *via* low pressure CVD using [$WSeCl_4(Se^nBu_2)$]. (a) XPS survey scan of binding energies in the range of 0 eV to 650 eV, with peaks related to the atomic orbitals of W (blue) and Se (orange) labelled. Elemental scans for the as-deposited WSe_2 film showing the peaks associated with W (b) and Se (c).

basis set as used for $WSeCl_4$. Energy minima were confirmed by the absence of any imaginary frequencies using a frequency calculation and calculated frequencies were adjusted by standard scaling factors.[34]

Following the method of Britnell *et al.*,[21] freshly ground WCl_6 (6.19 g, 15.6 mmol) and Sb_2Se_3 (2.5 g, 5.2 mmol) were mixed in a glove box and added to a glass reaction tube (Fig. 14) under a dinitrogen atmosphere. The glass tube was then placed under vacuum and sealed with a gas torch at point (1). Section A was placed in a tube furnace at 120 °C for 4 days, with section C at room temperature, to allow the side products to deposit in the cooler section. This was then removed by sealing the glass at point (2). Section A was placed back in the furnace, with section B at room temperature for 4 days until more side product had collected in section B. At this point, joint (3) was broken in a glovebox and the solid remaining in section A removed and ground up, and the resulting green powder placed in a glass tube and heated at 170 °C for 6 h *in vacuo.* Any remaining $SbCl_3$ pumped away and a grey solid had sublimed in the glass tube, leaving a brown residue which was discarded. The grey solid was removed in a glovebox and ground up to afford a bright green solid. Yield: 4.3 g, 68%. IR spectrum (Nujol, cm^{-1}): 377 W═Se, 367, 353, 336 W–Cl.

[$WSeCl_4$(MeCN)]. MeCN (0.3 mL) in CS_2 (2 mL) was added to a green suspension of $WSeCl_4$ (0.150 g, 0.37 mmol) in CS_2 (5 mL). The resulting bright green suspension was stirred for 20 min and concentrated to 50% volume before the mother liquor was removed by filtration, to obtain a green powder, which was dried *in vacuo*. Yield: 0.125 g, 76%. Required for $C_2H_3Cl_4NSeW$ (445.66): C, 5.39; H, 0.68; N, 3.14. Found: C, 5.51; H, 1.03; N, 2.90%. IR spectrum (Nujol, cm^{-1}): 2308 C═N, 2281, ν(C–C) + $\delta(CH_3)$, 373 W═Se, 347, 332 W–Cl. ^{1}H NMR (CD_2Cl_2): δ = 2.30 (s). The same complex can be obtained using CH_2Cl_2 or C_6H_6 as solvent or neat MeCN.

[$WSeCl_4$(THF)]. THF (0.01 mL, 0.14 mmol) was added to a stirring solution of $WSeCl_4$ (0.060 g, 0.14 mmol) in benzene (2 mL). The resulting green solution was frozen in liquid nitrogen, then allowed to warm to *ca.* −5 °C and the benzene was sublimed under vacuum to leave a green solid. Yield: 0.045 g, 67%. Required for $C_4H_8Cl_4OSeW$ (476.72): C, 10.08; H 1.69. Found: C, 10.75; H, 1.80%. IR spectrum (Nujol, cm^{-1}): 1089, 846 thf, 373 W═Se, 344, 330 W–Cl. ^{1}H NMR (CD_2Cl_2): δ = 4.08 (s, [4H]), 1.96 (s, [4H]).

[$WSeCl_4(OPPh_3)$]. A solution of $OPPh_3$ (0.069 g, 0.2 mmol) in dichloromethane (5 mL) was added slowly to a suspension of $WSeCl_4$ (0.100 g, 0.2 mmol) in dichloromethane (5 mL). The resulting green solution was then stirred for 30 min, concentrated to ~1 mL *in vacuo*, filtered, and the resulting green solid washed with hexane (2 × 1 mL), and dried *in vacuo*. Yield: 0.105 g, 76%. Required for $C_{18}H_{15}Cl_4OPSeW$ (682.9): C, 31.66;

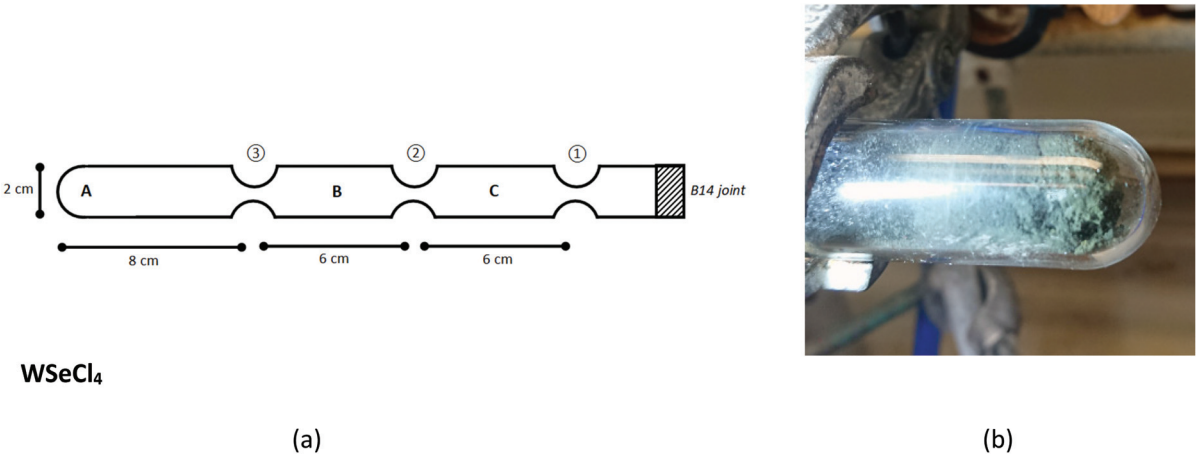

Fig. 14 (a) A borosilicate glass tube with three 1 cm constrictions, and a B14 joint, used for the solid-state reaction of WCl_6 and Sb_2Se_3 to form $WSeCl_4$; (b) grey-green solid remaining in the reaction tube after heating.

H, 2.21. Found: C, 31.86; H, 2.15%. IR spectrum (Nujol, cm^{-1}): 1131 P═O, 360 W═Se, 337, 309 W–Cl. ^1H NMR (CD_2Cl_2): δ = 7.77 (m, [6H]), 7.67 (m, [3H]), 7.63 (m, [6H]). $^{31}P\{^1H\}$ NMR (CD_2Cl_2): δ = +45.7 (s). The same complex was obtained using C_6H_6, toluene or CS_2 as solvent or by reaction of $OPPh_3$ with [$WSeCl_4$(MeCN)] in a 1 : 1 molar ratio.

[$WSeCl_4$(DMF)]. DMF (0.019 mL, 0.25 mmol) was added to a stirring solution of $WSeCl_4$ (0.100 g, 0.25 mmol) in benzene (2 mL). The resulting green solution was frozen in liquid nitrogen, before being allowed to warm to *ca.* −5 °C under dynamic vacuum to remove the benzene *via* sublimation to afford a green solid. The complex decomposes in a few hours even in the glove box, therefore a satisfactory microanalysis could not be obtained, and it was identified by a single crystal X-ray structure determination. Yield: 0.080 g, 66%. IR spectrum (Nujol, cm^{-1}): 1644 C═O, 388 W═Se, 367, 331 W–Cl. ^1H NMR (C_6D_6): δ = 7.57 (s, [H]), 1.89 (s, [3H]), 1.35 (s, [3H]).

[$WSeCl_4$(2,2′-bipy)]. 2,2′-Bipy (0.039 g, 0.25 mmol) in toluene (3 mL) was added slowly to a purple suspension of $WSeCl_4$ (0.100 g, 0.25 mmol) in toluene (4 mL). The red suspension was stirred for 10 min, before the colourless solution was filtered off the red/brown solid, which was washed in CH_2Cl_2 (1 mL) and dried *in vacuo*. Yield: 0.090 g, 56%. Required for $C_{10}H_8Cl_4N_2SeW{\cdot}CH_2Cl_2$ (645.73): C, 20.46; H, 1.56; N, 4.34. Found: C, 20.36; H, 1.61; N, 5.50%. IR spectrum (Nujol, cm^{-1}): 341 W═Se, 313 W–Cl. ^1H NMR (CD_2Cl_2): δ = 8.92 (d, [2H], J_{HH} = 4.7 Hz), 8.89 (d, [2H], J_{HH} = 8.2 Hz), 8.28 (dt, [2H], J_{HH} = 1.7, 7.8 Hz), 7.75 (dt, [2H], J_{HH} = 1.0, 6.8 Hz).

[$WSeCl_4(NC_5H_5)$]. Pyridine (0.020 g, 0.25 mmol) was added slowly to a purple suspension of $WSeCl_4$ (0.100 g, 0.25 mmol) in CH_2Cl_2 (5 mL). The resulting green suspension was stirred for 10 min before the volatiles were removed *in vacuo*, to afford a green-brown solid. Yield: 0.076 g, 63%. Required for $C_5H_5Cl_4NSeW$ (483.71): C, 12.42; H, 1.04; N, 2.90. Found C, 13.40; H, 1.54; N, 2.96%; see comment above regarding instability of the complexes. IR spectrum (Nujol, cm^{-1}): 364 W═Se, 327 W–Cl. ^1H NMR (CD_2Cl_2): δ = 8.65 (br [2H]), 8.25 (br, [1H]), 7.82 (br, [2H]).

[$(WSeCl_4)_2$(μ-4,4′bipy)]. A solution of 4,4′-bipy (0.013 g, 0.08 mmol) in CH_2Cl_2 (2 mL) was added to a stirring solution of [$WSeCl_4$(MeCN)] (0.075 g, 0.16 mmol) in CH_2Cl_2 (3 mL). The green suspension was stirred for 5 min before concentrating to approx. half the volume. The brown/green solid was isolated by filtration and dried *in vacuo*. Yield: 0.035 g, 45%. Required for $C_{10}H_8Cl_8N_2Se_2W_2$ (965.41): C, 12.44; H, 0.81, N, 2.90. Found: C, 12.23; H, 2.00, N, 2.74%. IR spectrum (Nujol, cm^{-1}): 365 W═Se, 333 W–Cl. ^1H NMR (CD_2Cl_2): δ = 9.20 (m, [4H]), 7.74 (m, [4H]).

[$(WSeCl_4)_2$(1,4-dioxane)]. 1,4 dioxane (0.01 mL, 0.13 mmol) was added to a stirring solution of $WSeCl_4$ (0.100 g, 0.25 mmol) in CH_2Cl_2 (2 mL). The green solution was stirred for 5 min before the volatiles were removed under vacuum to afford a green solid. Yield: 0.082 g, 70%. Required for $C_4H_8Cl_8O_2Se_2W_2$ (897.33): C, 5.35; H, 0.90. Found: C, 4.50; H, 1.15%. IR spectrum (Nujol, cm^{-1}): 377 W═Se, 361, 333 W–Cl. ^1H NMR (C_6D_6): δ = 3.47 (s).

[$(WSeCl_4)_2$(μ-dppmO_2)]. A solution of dppmO_2 (0.053g, 0.125 mmol) in CH_2Cl_2 (3 mL) was added to a stirring suspension of $WSeCl_4$ (0.100 g, 0.25 mmol) in CH_2Cl_2 (3 mL) to give a green-brown suspension. After 5 min the brown solution was filtered away and the remaining green solid was dried *in vacuo*. Yield: 0.083 g, 54%. Required for $C_{25}H_{22}Cl_8O_2P_2Se_2W_2$ (1225.61): C, 24.5; H, 1.81. Found: C, 25.5; H, 1.94%. IR spectrum (Nujol, cm^{-1}): 1074 P═O, 366 W═Se, 338, 337 W–Cl. ^1H NMR (C_6D_6): δ = 7.80 (m, [8H]), 7.61 (m, [4H]), 6.90 (m, [8H]), 4.64 (t, [2H], $^2J_{H-P}$ = 15.6 Hz). $^{31}P\{^1H\}$ NMR (C_6D_6): δ = +45.9 (s). The product was very poorly soluble and the dilute solution showed significant decomposition, therefore solution data were collected *in situ*, but also show some decomposition.

[$WSeCl_4(SeMe_2)$]. A solution of $SeMe_2$ (0.016 g, 0.15 mmol) in benzene (1 mL) was added to a stirring solution of $WSeCl_4$ (0.060 g, 0.15 mmol) in benzene (2 mL) forming a green/black

suspension. After 5 min the solvent was removed *in vacuo* to give a red/brown sticky solid. Yield: 0.035 g, 46%. Required for $C_2H_6Cl_4Se_2W$ (513.64): C, 4.68; H, 1.18. Found: C, 4.67; H, 1.42%. IR spectrum (Nujol, cm^{-1}): 371 W═Se, 344 W–Cl. ^1H NMR (CD_2Cl_2): 1.41 (br s, [6H]).

[$WSeCl_4(Se^nBu_2)$]. A solution of Se^nBu_2 (0.047 g 0.24 mmol) in benzene (1 mL) was added to a stirring solution of $WSeCl_4$ (0.1 g, 0.24 mmol) in benzene (2 mL) forming a green/black suspension. After 5 min the solvent was removed *in vacuo* to give a viscous red oil, which was not sufficiently stable to obtain (out-sourced) microanalytical measurements. IR spectrum (Nujol, cm^{-1}): 380 W═Se, 352, 321 W–Cl. ^1H NMR (*in situ* in C_6D_6): 2.48 (t, J = 7.6 Hz, [2H] CH_2), 1.46 (m, [2H], CH_2), 1.17 (m, [2H] CH_2), 0.73 (t, J = 7.3 Hz, [3], CH_3). $^{77}Se\{^1H\}$ NMR (CD_2Cl_2, 295 K): δ = 292; (183 K): δ = 295.

LPCVD growth of WSe_2 films using [$WSeCl_4(Se^nBu_2)$]

The precursor (50–60 mg) was loaded into the precursor bulb at the closed end of a silica tube in a N_2 purged glove box, silica substrates (*ca.* 1 × 8 × 20 mm^3) were then positioned end-to-end lengthways along the tube away from the precursor. The tube was then set horizontally in a furnace so that the substrates were in the hot zone and the precursor protruded *ca.* 4 cm beyond the end of the tube furnace. The tube was evacuated to 0.1 mm Hg and the furnace heated to 700 °C and left for 15 min to allow the temperature to stabilise. The tube was gradually moved towards the hot zone until evaporation of the precursor began and the position was maintained until no further evaporation occurred, leaving a small amount of dark sticky residue in the precursor bulb. After *ca.* 10 min the tube was cooled to room temperature and the substrates were removed and stored for characterisation. Uniformly shiny silver films were observed on the substrates from the hot zone at temperatures between 650–700 °C (determined by temperature profiling), *i.e.* 8–18 cm away from the precursor.

Film characterisation

X-ray diffraction (XRD) patterns were collected in grazing incidence mode (θ_1 = 1°) using a Rigaku SmartLab diffractometer (Cu-K_α, λ = 1.5418 Å) with parallel X-ray beam and a Hypix detector operated in 1D mode. Phase matching and lattice parameter calculations (WS_2) used the PDXL2 software package[55] and diffraction patterns from ICSD.[56] High resolution scanning electron microscopy (SEM) measurements were carried out with a field emission SEM (Jeol JSM 7500F) at an accelerating voltage of 2 kV. X-ray photoelectron spectroscopy (XPS) data were obtained using a ThermoScientific Theta Probe system with Al-K_α radiation (photon energy = 1486.6 eV). All peaks are calibrated against the adventitious C 1s peak at 284.6 eV. Raman spectra of the deposited films were measured at room temperature on a Renishaw InVia Micro Raman Spectrometer using 532 nm excitation. The incident laser power was adjusted to 0.1 mW for all samples.

Conclusions

Single crystal and powder XRD data for $WSeCl_4$ reveal discrete square pyramidal monomers, which contrasts with the weakly chloride bridged dimer and tetramer units in $WSCl_4$, while $WOCl_4$ is a strongly oxido-bridged polymer.[3,57] The weaker Lewis acidity of $WSeCl_4$ that this implies, is supported by DFT calculations and is also manifest in its coordination chemistry with neutral ligands. The synthesis and spectroscopic characterisation of the first extended series of complexes with neutral N-, O- and Se- donor ligands are described, which, with the exception of the seven-coordinate [$WSeCl_4$(2,2′-bipy)], contain six-coordinate tungsten with the neutral donor *trans* to the W═Se. The structures were confirmed by six single crystal X-ray studies, the first on $WSeCl_4$ complexes. In contrast to the behaviour with $WSCl_4$ and $WOCl_4$,[8] alkyl phosphines abstract Se from $WSeCl_4$ upon contact. The complexes of $WSeCl_4$ are less robust both in solution and in the solid state compared to those of $WSCl_4$ and $WOCl_4$, with some decomposing rapidly in solution.

Notably, despite its limited solution stability, [$WSeCl_4(Se^nBu_2)$] has been shown to function as a very effective LPCVD reagent for the deposition of thin films of the key WSe_2 semiconductor; the first example of a single source precursor for this technologically important material. The resulting films were characterised by grazing incidence X-ray diffraction and scanning electron microscopy, both of which indicate very strong preferred growth in the <00*l*> direction, together with XPS and Raman spectroscopy. Further work focusing on optimising the film deposition and to explore the electrical properties of these CVD grown films is underway.

In contrast to the behaviour of [$WSCl_4$(L)] analogues, the [$WSeCl_4$(L)] generally do not lead to complexes of W(v), [$WSeCl_3$(L)], on standing either at ambient temperature, by heating in solution, or by reaction with excess L. A few crystals of one W(v) example, [{$WCl_3(SMe_2)$}$_2$(μ-Se)(μ-Se_2)], were isolated from the attempted preparation of [$WSeCl_4(SMe_2)$].

Conflicts of interest

The authors have no conflicts to declare.

Acknowledgements

We thank EPSRC for support through EP/P025137/1 and the ADEPT Programme Grant (EP/N035437/1). We would also like to thank Prof. J. M. Dyke for helpful discussions regarding the DFT calculations reported herein. We wish to acknowledge the use of the EPSRC funded Physical Sciences Data-science Service hosted by the University of Southampton and STFC under grant number EP/S020357/1.

References

1 *Comprehensive Coordination Chemistry*, ed. G. Wilkinson, R. D. Gillard and J. A. McCleverty, Pergamon, Oxford, 1987, vol. 3.
2 *Comprehensive Coordination Chemistry II*, ed. J. A. McCleverty and T. J. Meyer, Elsevier, Oxford, 2003, vol. 4.
3 R. A. Walton, *Prog. Inorg. Chem.*, 1972, **16**, 1.
4 D. A. Rice, *Coord. Chem. Rev.*, 1978, **25**, 199.
5 V. K. Greenacre, W. Levason, G. Reid and D. E. Smith, *Coord. Chem. Rev.*, 2020, **424**, 213512.
6 W. Levason, F. M. Monzittu and G. Reid, *Coord. Chem. Rev.*, 2019, **391**, 90.
7 V. K. Greenacre, A. L. Hector, W. Levason, G. Reid, D. E. Smith and L. Sutcliffe, *Polyhedron*, 2019, **162**, 14.
8 W. Levason, G. Reid, D. E. Smith and W. Zhang, *Polyhedron*, 2020, **179**, 114372.
9 D. E. Smith, V. K. Greenacre, A. L. Hector, W. Levason, G. Reid, F. Robinson and S. Thomas, *Dalton Trans.*, 2020, **49**, 2496.
10 R. D. Bannister, W. Levason, M. E. Light, G. Reid and W. Zhang, *Polyhedron*, 2019, **167**, 1.
11 R. D. Bannister, W. Levason, G. Reid and F. Robinson, *Polyhedron*, 2019, **169**, 129.
12 Y.-P. Chang, A. L. Hector, W. Levason and G. Reid, *Dalton Trans.*, 2017, **46**, 9824.
13 *Chemical Vapour Deposition: Precursors, Processes and Applications*, ed. A. C. Jones and M. L. Hitchman, The Royal Society of Chemistry, 2009.
14 M. Chhowalla, Z. Liu and H. Zhang, *Chem. Soc. Rev.*, 2015, **44**, 2584 (ed. – themed issue on metal dichalcogenides).
15 M. Chhowalla, H. S. Shin, G. Eda, L.-J. Li, K. P. Loh and H. Zhang, *Nat. Chem.*, 2013, **5**, 263; J. Liu and X.-W. Liu, *Adv. Mater.*, 2012, **24**, 4097.
16 J. R. Brent, N. Savjani and P. O'Brien, *Prog. Mater. Sci.*, 2017, **89**, 411.
17 Q. Xiang, J. Yu and M. Jaroniec, *J. Am. Chem. Soc.*, 2012, **134**, 6575; K. Lee, R. Gatensby, N. McEvoy, T. Hallam and G. S. Duesberg, *Adv. Mater.*, 2013, **25**, 6699; K. Xu, P. Chen, X. Li, C. Wu, Y. Guo, J. Zhao, X. Wu and Y. Xie, *Angew. Chem., Int. Ed.*, 2013, **52**, 10477; Z. Yan, C. Jiang, T. R. Pope, C. F. Tsang, J. L. Stickney, P. Goli, J. Renteria, T. T. Salguero and A. A. Balandin, *J. Appl. Phys.*, 2013, **114**, 20430.
18 S. L. Benjamin, C. H. de Groot, C. Gurnani, A. L. Hector, R. Huang, K. Ignatyev, W. Levason, S. J. Pearce, F. Thomas and G. Reid, *Chem. Mater.*, 2013, **25**, 4719.
19 M. D. Khan, M. A. Malik and N. Revaprasadu, *Coord. Chem. Rev.*, 2019, **388**, 24.
20 V. Brune, M. Grisch, R. Weißing, F. Hartle, M. Frank, S. Mishra and S. Mathur, *Dalton Trans.*, 2021, **50**, 12365.
21 D. Britnell, G. W. A. Fowles and D. A. Rice, *J. Chem. Soc., Dalton Trans.*, 1974, 2191.
22 M. G. B. Drew, E. M. Page and D. A. Rice, *J. Chem. Soc., Dalton Trans.*, 1983, 61.
23 D. Britnell, G. W. A. Fowles and D. A. Rice, *J. Chem. Soc., Dalton Trans.*, 1975, 213.
24 G. W. A. Fowles, D. A. Rice and K. J. Shanton, *J. Chem. Soc., Dalton Trans.*, 1978, 1658.
25 N. D. Boscher, C. J. Carmalt and I. P. Parkin, *J. Mater. Chem.*, 2006, **16**, 122.
26 V. C. Gibson, T. P. Kee and A. Shaw, *Polyhedron*, 1990, **9**, 2293.
27 U. Müller and P. Klingelhöfer, *Z. Anorg. Allg. Chem.*, 1984, **510**, 109.
28 M. G. B. Drew and R. Mandyczewky, *J. Chem. Soc. A*, 1970, 2815.
29 F. A. Cotton, P. A. Kibala and R. B. W. Sandor, *Inorg. Chem.*, 1989, **28**, 2485.
30 D. L. Hughes, J. D. Lane and R. L. Richards, *J. Chem. Soc., Dalton Trans.*, 1991, 1627.
31 E. M. Page, D. A. Rice, K. Hagen, L. Hedberg and K. Hedberg, *Inorg. Chem.*, 1982, **21**, 3280.
32 P. J. Jones, W. Levason, J. S. Ogden, J. W. Turff, E. M. Page and D. A. Rice, *J. Chem. Soc., Dalton Trans.*, 1983, 2625.
33 (*a*) S. Grimme, *J. Comput. Chem.*, 2006, **27**, 1787; (*b*) S. Grimme, S. Ehrlich and L. Goerigk, *J. Comput. Chem.*, 2011, **32**, 1456; (*c*) C. Lee, W. Yang and R. G. Parr, *Phys. Rev. B: Condens. Matter Mater. Phys.*, 1988, **37**, 785; (*d*) P. J. Stephens, F. J. Devlin, C. F. Chabalowski and M. J. Frisch, *J. Phys. Chem.*, 1994, **98**, 11623.
34 From https://cccbdb.nist.gov/vibscalejust.asp, Computational Chemistry Comparison and Benchmark Database.
35 J. W. Emsley, W. Levason, G. Reid, W. Zhang and G. De Luca, *J. Fluorine Chem.*, 2017, **197**, 74.
36 M. G. B. Drew, G. W. A. Fowles, E. M. Page and D. A. Rice, *J. Chem. Soc., Dalton Trans.*, 1981, 2409.
37 P. Klingelhöfer and U. Müller, *Z. Anorg. Allg. Chem.*, 1988, **536**, 70.
38 W. McFarlane and D. S. Rycroft, *J. Chem. Soc., Dalton Trans.*, 1973, 2162.
39 N. Muller, P. C. Lauterbur and J. Goldenson, *J. Am. Chem. Soc.*, 1956, **78**, 3556.
40 M. G. B. Drew, E. M. Page and D. A. Rice, *J. Chem. Soc., Dalton Trans.*, 1983, 61.
41 W. Levason, S. D. Orchard and G. Reid, *Coord. Chem. Rev.*, 2002, **225**, 159.
42 M. G. B. Drew, D. A. Rice and D. M. Williams, *J. Chem. Soc., Dalton Trans.*, 1983, 2251.
43 M. G. B. Drew, D. A. Rice and D. M. Williams, *J. Chem. Soc., Dalton Trans.*, 1984, 1087.
44 J. A. Champion, *Br. J. Appl. Phys.*, 1965, **16**, 1035.
45 W. Zhao, Z. Ghorannevis, K. K. Amara, J. R. Pang, M. Toh, X. Zhang, C. Kloc, P. H. Tan and G. Eda, *Nanoscale*, 2013, **5**, 9677.
46 H. Zeng, G.-B. Liu, J. Dai, Y. Yan, B. Zhu, R. He, L. Xie, S. Xu, X. Chen, W. Yao and X. Cui, *Sci. Rep.*, 2013, **3**, 1608.
47 Y. Q. Ma, B. L. Liu, A. Y. Zhang, L. Chen, M. Fathi, A. Abbas, M. Y. Ge, C. F. Shen and C. W. Zhou, *ACS Nano*, 2015, **9**, 7383.

48 X. Wang, X. Chen, Y. Zhou, C. Park, C. An, Y. Zhou, R. Zhang, C. Gu, W. Yang and Z. Yang, *Sci. Rep.*, 2017, 46694.
49 X. Zhang, W. P. Han, J. B. Wu, S. Milana, Y. Lu, Q. Q. Li, A. C. Ferrari and P. H. Tan, *Phys. Rev. B: Condens. Matter Mater. Phys.*, 2013, **87**, 115413.
50 Y. Zhao, X. Luo, H. Li, J. Zhang, P. T. Araujo, C. K. Gan, J. Wu, H. Zhang, S. Y. Quek, M. S. Dresselhaus and Q. Xiong, *Nano Lett.*, 2013, **13**, 1007.
51 R. Zhang, D. Drysdale, V. Koutsos and R. Cheung, *Adv. Funct. Mater.*, 2017, 1702455.
52 W. Levason, R. Patel and G. Reid, *J. Organomet. Chem.*, 2003, **688**, 280.
53 (*a*) G. M. Sheldrick, *Acta Crystallogr., Sect. C: Struct. Chem.*, 2015, **71**, 3; (*b*) G. M. Sheldrick, *Acta Crystallogr., Sect. A: Found. Crystallogr.*, 2008, **64**, 112; (*c*) O. V. Dolomanov, L. J. Bourhis, R. J. Gildea, J. A. K. Howard and H. Puschmann, *J. Appl. Crystallogr.*, 2009, **42**, 339.
54 M. J. Frisch, G. W. Trucks, H. B. Schlegel, G. E. Scuseria, M. A. Robb, J. R. Cheeseman, G. Scalmani, V. Barone, G. A. Petersson, H. Nakatsuji, X. Li, M. Caricato, A. V. Marenich, J. Bloino, B. G. Janesko, R. Gomperts, B. Mennucci, H. P. Hratchian, J. V. Ortiz, A. F. Izmaylov, J. L. Sonnenberg, D. Williams-Young, F. Ding, F. Lipparini, F. Egidi, J. Goings, B. Peng, A. Petrone, T. Henderson, D. Ranasinghe, V. G. Zakrzewski, J. Gao, N. Rega, G. Zheng, W. Liang, M. Hada, M. Ehara, K. Toyota, R. Fukuda, J. Hasegawa, M. Ishida, T. Nakajima, Y. Honda, O. Kitao, H. Nakai, T. Vreven, K. Throssell, J. A. Montgomery Jr., J. E. Peralta, F. Ogliaro, M. J. Bearpark, J. J. Heyd, E. N. Brothers, K. N. Kudin, V. N. Staroverov, T. A. Keith, R. Kobayashi, J. Normand, K. Raghavachari, A. P. Rendell, J. C. Burant, S. S. Iyengar, J. Tomasi, M. Cossi, J. M. Millam, M. Klene, C. Adamo, R. Cammi, J. W. Ochterski, R. L. Martin, K. Morokuma, O. Farkas, J. B. Foresman and D. J. Fox, *Gaussian 16, Revision C.01*, Gaussian, Inc., Wallingford, CT, 2016.
55 S. Grazulis, D. Chateigner, R. T. Downs, A. F. Yokochi, M. Quiros, L. Lutterotti, E. Manakova, J. Butkus, P. Moeck and A. Le Bail, *J. Appl. Crystallogr.*, 2009, **42**, 726.
56 ICSD: Inorganic Crystal Structure Database (ICSD) accessed via the EPSRC funded Physical Sciences Data-science Service hosted by the University of Southampton and STFC.
57 H. Hess and H. Hartung, *Z. Anorg. Allg. Chem.*, 1966, **344**, 157.